Simultaneous quantification of liver perfusion and hepatocyte uptake function with dynamic gadoxetate-enhanced MR imaging in patients with chronic liver diseases

Benjamin Leporq[1], Sabine Schmidt[2], Catherine Pastor[1,3], Jean Luc Daire[1], and Bernard Edgar Van Beers[1,4]

[1]*Center of research on inflammation, Paris 7 University; INSERM U1044, Paris, France,* [2]*Department of Radiology, Centre Hospitalier Universitaire Vaudois, Lausanne, Switzerland,* [3]*Laboratoire de Physiopathologie Hépatique et Imagerie Moléculaire, Hôpitaux Universitaires de Genève, Geneva, Switzerland,* [4]*Department of Radiology, Beaujon University hospital Paris Nord, Clichy, France*

Introduction: Assessment of liver function is important to determine the prognosis of patients with chronic liver diseases, and is particularly required in patients with cirrhosis to define the optimal timing for transplantation. Evaluation of total and regional liver function is also needed before major liver resection to minimize the risk of post-operative liver failure (1). The aim of this study was to evaluate the feasibility of quantifying simultaneously the liver perfusion and hepatocyte uptake function with dynamic gadoxetate-enhanced MR imaging. The feasibility was prospectively assessed in patients with liver chronic diseases and healthy volunteers.

Material and Method: ***MR dynamic acquisition*** **-** A 3D TWIST sequence was used on a Siemens Skyra 3.0T system. Acquisition parameters were: central region A, 40 %; sampling density B, 50 %; GRAPPA, 3×1; TE/TR/α, 0.84 ms/2.44 ms/15°; oversampling, 20 and 10% according to phase and slice direction; k-space partial filling, 6/8th and 745 Hz.pixel^{-1} BW. The acquisition plane was coronal with right/left phase encoding direction and a 1.875×1.875×3 mm^3 spatial resolution. Forty slices covered the whole liver with a temporal resolution of 2.08 s. Gadoxetate (0.025 mmol.kg^{-1}) was injected at a rate of 1 mL.s^{-1}. ***Image processing*** **-** An in-house application running on Matlab R2012b (The Mathworks, Natick, MA, USA) was developed. First, to compensate for misregistrations between dynamic images each 2D+t stack of images were registered with an iconic approach using a rigid motion as a search space and the minimization of the mutual information of the normalized joint histogram as a similarity function. The kinetic of gadoxetate was modeled with a dual input two-compartment uptake model as reported by Sourbron et al. (2), giving the following relation: $C_t(t) = \phi_a C_a(t-\tau_A) + \phi_p C_p(t-\tau_P) \otimes \left[e^{-\frac{t}{MTTe}} + E(1-e^{-\frac{t}{MTTe}})\right]$. $C_t(t)$, $C_a(t)$ and $C_p(t)$ were the tissue impulse response, the arterial input and portal input functions respectively. τ_a and τ_p are the arterial and portal delays, Φ_a and Φ_p are the arterial and portal perfusions, MTT_e the extracellular mean transit time and E the uptake fraction. Signal intensity was converted into relative tracer concentration (C) according to $C(t) = (S(t)-S_0)/S_0$. Tissue impulse response, arterial and portal input were recorded through the mean value measured from regions of interest placed on the liver, the abdominal aorta and the main portal trunk, and were interpolated with spline curves. Arterial delay was fixed as the temporal difference between the arterial input function and the tissue impulse response enhancements. The variables τ_p, Φ_a, Φ_p, MTT_e and E were derived from a non-linear least square fit on the tissue impulse response. The fitting procedure was performed with a multistart (50 runs) constrained trust region reflective algorithm. **Subjects**: Fifteen patients with chronic liver diseases and METAVIR fibrosis scores of F0 – F4 at histopathology, as well as 6 healthy volunteers were prospectively enrolled.

Results: Based on the histological results, 3 groups were grouped together: a group without fibrosis including 8 healthy volunteers and F0 patients; a fibrosis group including 10 patients scored F1 to F3 and a cirrhosis group including 3 patients with F4 stage. The arterial perfusion increased significantly between the three groups ($p < 0.05$) whereas portal perfusion decreased leading to an increase of the arterial fraction (hepatic perfusion index, HPI) between the fibrosis and cirrhosis groups. The hepatocyte uptake fraction and uptake flow rate decreased significantly between the no fibrosis and fibrosis groups ($p < 0.01$) and between the fibrosis and cirrhosis groups ($p < 0.05$).

	No fibrosis (n=8)	**Fibrosis (n=10)**	**Cirrhosis (n=3)**
Arterial perfusion *(mL.min^{-1}.100g^{-1})*	10.4 ± 7.6	20.0 ± 11.2	58.6 ± 32.2
Portal perfusion *(mL.min^{-1}.100g^{-1})*	39.1 ± 10.4	52.1 ± 21.4	25.5 ± 23.6
Hepatic perfusion index *(%)*	21.2 ± 15.9	29.0 ± 15.9	67.6 ± 30.1
MTT_e *(s)*	23.9 ± 5.9	15.1 ± 3.3	19.4 ± 4.4
RBV *(mL.100g^{-1})*	22.1 ± 4.8	19.7 ± 5.5	28.0 ± 7.7
Hepatocyte uptake fraction *(%)*	12.9 ± 5.0	6.9 ± 2.4	2.5 ± 3.7
Hepatocyte uptake flow rate *(mL.min^{-1}.100g^{-1})*	7.3 ± 3.3	5.3 ± 2.4	2.1 ± 3.1

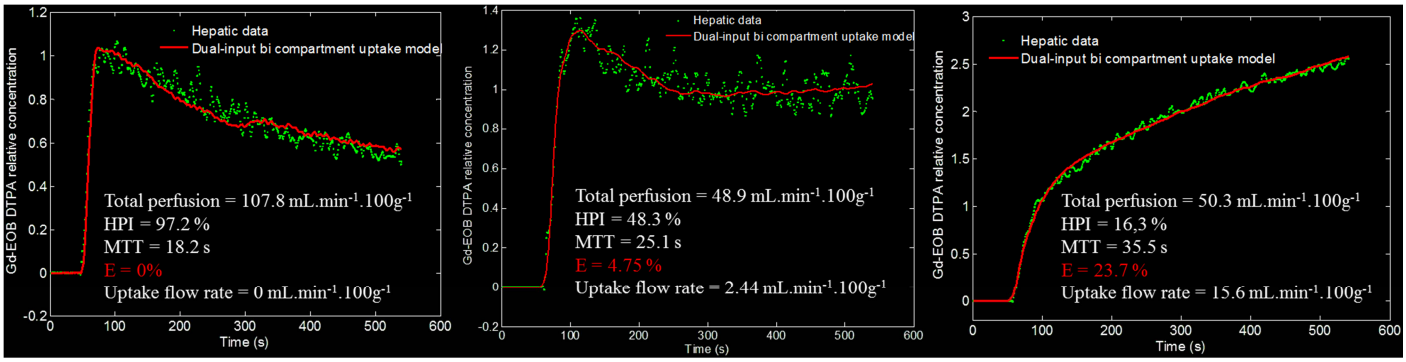

Fig.1*: Data fit on the tissue impulse response measured in a patient with cirrhosis (left panel), with F2 fibrosis (middle panel) and in a healthy volunteer (right panel). These results illustrate the gadoxetate uptake differences according to liver damage.*

Conclusion: Our preliminary results show both increase of hepatic artery fraction of liver perfusion and decrease of hepatocyte gadoxetate uptake in patients with chronic liver diseases, in accordance with previous studies assessing perfusion and hepatocyte uptake separately (Annet 2003, Lagadec 2014). In contrast to the deconvolution approach proposed by Nilsson *et al* (3), compartmental modeling as used here takes into account both arterial and portal inputs. This issue is very important since the arterial perfusion fraction changes according to disease severity. It is concluded that pharmacokinetic parameters at dynamic gadoxetate-enhanced MR imaging have the potential to become imaging biomarkers of both liver perfusion and hepatocyte function in patients with chronic liver diseases.

(1) de Graaf W *et al*. J Nucl Med 2010; 51:742-52. (2) Sourbron S et al. Radiology 2012;263:874-83. (3) Nilsson H *et al*. J Magn Reson Imaging 2009;29:1323-31.